Experimental spray characterisation of air-assisted impinging jets

A. Madan Mohan*[1], T. N. C. Anand [2], R. V. Ravikrishna[1]
[1] Dept. of Mechanical Engineering, Indian Institute of Science, India
[2] Dept. of Mechanical Engineering, Indian Institute of Technology Madras, India
ammohan@mecheng.iisc.ernet.in, anand@iitm.ac.in, and ravikris@mecheng.iisc.ernet.in

Abstract

Liquid atomization is a problem with applications in many fields. In the present study, an air-assisted impinging jet atomizer has been utilised and its spray characteristics have been studied at various conditions, using water as the liquid and nitrogen as the atomizing gas. Two configurations were studied: one having a central gas jet above two impinging liquid jets, and another having a central liquid jet targeted by two inclined gas jets. Backlit imaging and particle/droplet imaging and analysis techniques were utilised to characterise the sprays. It was observed that the configuration with a central gas jet and impinging liquid jets resulted in better atomization that the other case. It was observed that both the breakup length of the sheet and the resulting droplet sizes, reduced with an increase in the gas flow rate. The diameter of the gas jet orifice was also found to play an important role in changing the spread of the spray, the droplet sizes, and the radial distribution of droplet sizes. Overall, it is observed that by varying the gas-to-liquid ratio and nozzle orifices, it is possible to obtain a fine atomization of the spray using the air-assisted impinging jet configuration even at low injection pressures of below 0.4 MPa.

Introduction

Air-assisted atomization, in which kinetic energy of air is used to aid liquid breakup, has been used to atomize various kinds of liquids [1], [2], [3]. In most of these studies, either an annular/central liquid sheet is blasted with air jets, or gas is allowed to mix with the liquid inside the atomizer to form a spray. This method requires a large amount of gas to achieve droplet sizes of the order of 50 μm. Beck et al. [4] achieved a Sauter mean diameter (SMD) of 75 μm with water at a gas to liquid ratio (GLR) of the order of 1.0. On the other hand, impinging jet atomization has been used in rocket engines due to its good atomization and mixing characteristics [5], [6]. Impinging jet experiments with water by Shen et al. [7] showed that jet velocities of the order of 12.5 m/s was required to obtain an SMD in the range of 300 μm. In the present study, a liquid sheet is formed using two impinging liquid jets, and an air jet is directed on to this sheet to aid the atomization process. This combined effect of impinging jet and air assisted atomization helps in achieving smaller droplets at low liquid injection velocities.

Experimental Setup and Methods

The experimental setup consists of two parts, a liquid and gas supply system to the atomizer, and the optical setup to measure spray characteristics. In the supply system, high pressure nitrogen from a gas bottle is regulated to the gas reservoir tank and part of it is used to compress the liquid in the liquid reservoir. Liquid and gas flow rates are controlled using needle valves in their respective lines. The gas flow rate is measured using a thermal mass flow meter, while the liquid flow is measured using a gear flow meter. Digital pressure gages placed close to the atomizer measure the injection pressure. The spray is injected in a quiescent ambient condition. The spray is collected into a tank with a small exhaust fan at the bottom which creates sufficient suction to remove the mist without affecting the spray. The atomizer used in the present study consists of two liquid nozzles with an orifice of 0.76 mm in diameter, and a gas nozzle with an orifice diameter of 1.1 mm. The gas jet is placed over the impinging point of liquid jets at a distance of 7 mm, and making equal angles with them. The liquid jets impinge and form a liquid sheet in the plane perpendicular to that containing the axes of the injectors, and the gas supplied through the gas orifice is used to assist in the break-up of this sheet.

The optical setup for spray characteristic measurements is based on the backlit direct imaging method. It uses a pulsed Nd:YAG laser along with a fluorescent diffuser as a light source to back-illuminate the spray, and a CCD camera with a resolution of 2048 X 2048 pixels to record the spray images. A pulse duration of around 10 ns is used. The schematic of the experimental setup is shown in Fig. 1. In the present study, two types of image-based measurements are performed, one to study the spray structure and the other for droplet size measurements. For the spray structure measurements, images are taken from the exit of the orifice to 80 mm downstream. Small portions of the spray are imaged using a long distance microscope for droplet size measurements.

*Corresponding author: ammohan@mecheng.iisc.ernet.in

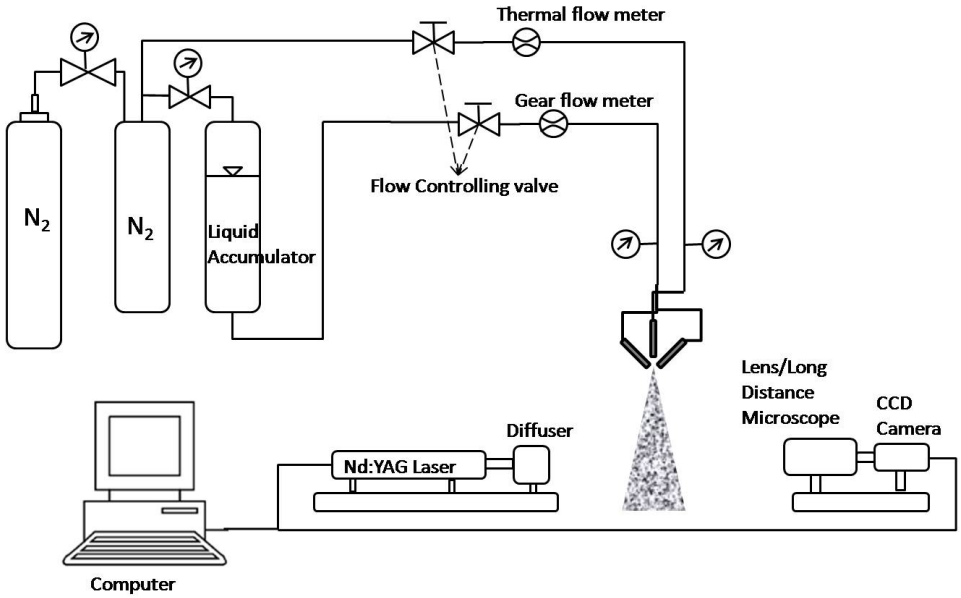

Figure 1. Experimental setup for spray structure visualization and droplet size measurement.

Particle/Droplet Imaging Analysis (PDIA)

Particle/Droplet Imaging Analysis (PDIA), an image-based, non intrusive droplet size measurement technique is used for droplet size measurements. In this method, back lit spray images are taken by zooming into a small area, and are analysed using computer based algorithms. Although this method was first reported in 1970's by Yule et al. [8], significant improvements to the algorithm were made in 1990's by Kim et al. [9] and Koh et al. [10]. This technique has been used extensively for particle/droplet size measurements in recent times due to developments in computational algorithms and technological improvements in digital imaging equipment. Use of short duration flash lights and lasers with a pulse width of the order 10 ns has extended the applicability of this method to high velocity sprays like diesel [11] and gasoline sprays [12]. Studies by Kashdan et al. [13] and Esmail et al. [12] have shown that PDIA measurements compare well with light-scattering based techniques such as Phase Doppler Anemometry (PDA). When compared with light-scattering based techniques like PDPA, PDIA has additional advantages of acquiring a visual record of the droplets measured, particle shape information, measuring non-spherical droplets accurately, and comparatively lower cost [13]. PDIA is a planar imaging technique and hence measures droplets for which the depth of focus (DOF) is different (the DOF is higher for larger droplets compared to smaller droplets). According to Kim et al. [9], the depth of focus varies linearly with droplet size. Further, a DOF correction can be applied to droplet statistics to minimize the error in the droplet distribution due to a variation in depth of focus [15].

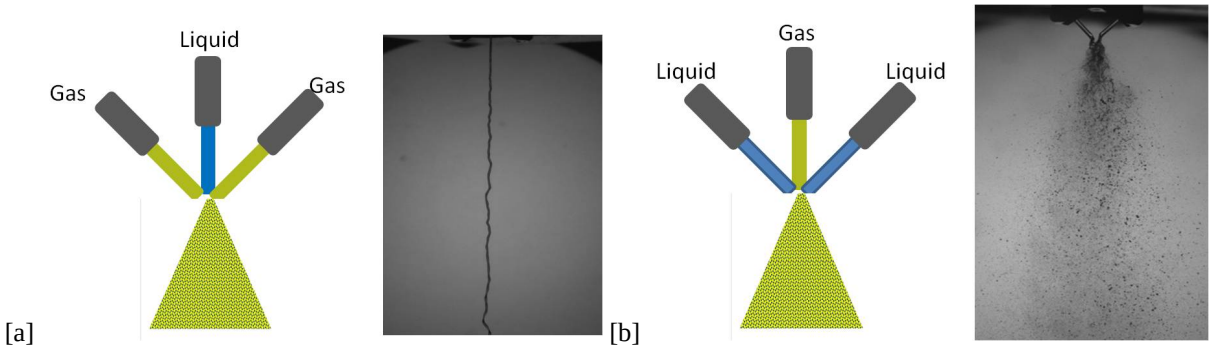

Figure 2. Spray structure of (a) Conventional air blast mode (b) Impinging air blast mode at same gas and liquid flow rates.

Table 1. Experimental conditions

Liquid flow rate $[LPM]$	Velocity $[m/s]$	Reynolds number	Weber number	GLR @ 5 SLPM	GLR @ 10 SLPM
0.1	1.8	1378	35	0.061	0.121
0.15	2.7	2067	78	0.040	0.081
0.2	3.6	2756	139	0.03	0.061
0.25	4.5	3445	217	0.024	0.048
0.3	5.4	4134	312	0.02	0.04
0.35	6.4	4823	425	0.017	0.035
0.4	7.3	5512	555	0.015	0.03

Results and Discussion

In the present study, air-assisted impinging-jet spray characteristics are studied using water as the liquid and nitrogen as the atomizing gas. Spray structure images were taken at three different liquid jet impinging angles viz. 60°, 90° and 120°, and the gas flow rates were varied at each impingement angle. The liquid jet velocity was between 1.8 m/s and 7.3 m/s at each impingement angle and the gas flow rate between 0 and 10 standard liters per minute (SLPM). The experimental conditions used in the current study are shown in Table 1. To compare conventional airblast atomization with the present method, spray images at the same liquid and gas flow rates are obtained for both configurations, and are shown in Fig. 2. With the conventional method, it is observed that an unbroken liquid jet exists with wavy patterns created by the gas impingement on to it. By swapping the air and liquid jet positions and thereby placing the gas jet between the liquid jets, it is observed that the liquid jets break up completely and form a spray.

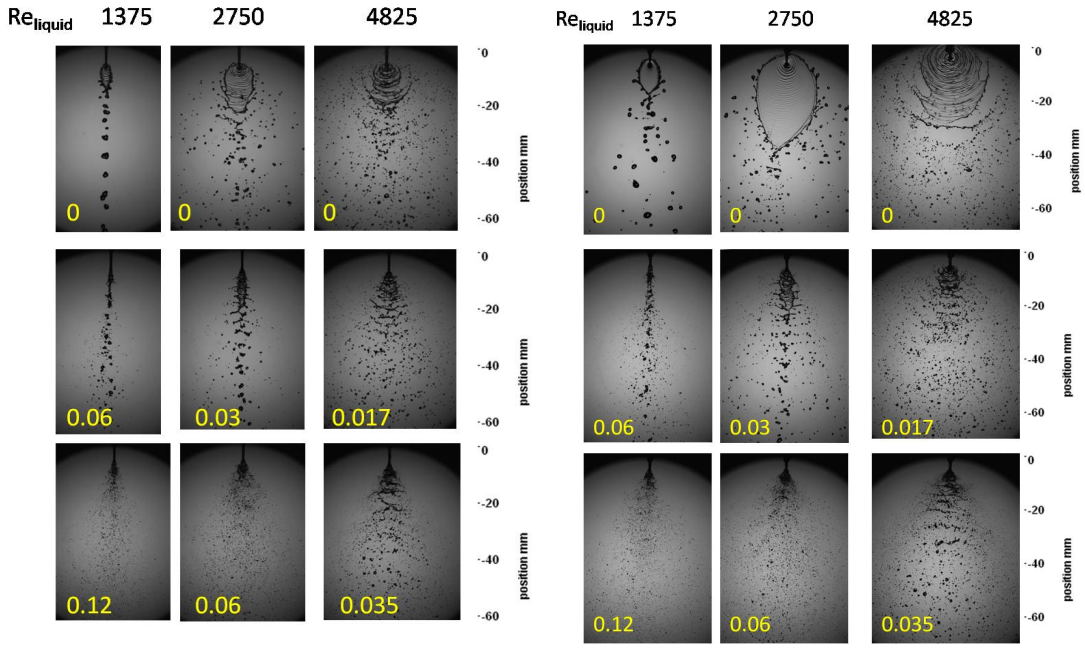

Figure 3. Spray structure at different Gas to Liquid Ratios (GLRs) and impinging angle of (a) 90°, and (b) 120°.

Spray structure images are taken using the backlit direct imaging technique described earlier, at a rate of 10 frames per second. Instantaneous spray images at different conditions are shown in Fig. 3. The spray structure at an impinging angle of 90° is shown in Fig. 3 (a) while Fig. 3 (b) shows the structure at an impinging angle of 120°. The gas to liquid ratio (GLR) at each condition is mentioned on the image. With pure impinging liquid jets, without a gas jet, liquid sheets break up due to impact waves. At low liquid jet velocities, increasing the liquid jet velocity results in an increase in the liquid sheet size and droplets are pinched off the from the sheet edges. A further increase in the velocity creates impact waves which break the sheet rapidly. Introducing gas on top of the impinging point enhances the instabilities on the sheet and results in a faster breakup. It is observed that increasing the gas flow rate further improves the breakup by a large extent, especially at low liquid velocities. It is also observed that the spread of the spray in the lateral direction is reduced with the introduction of the gas jet.

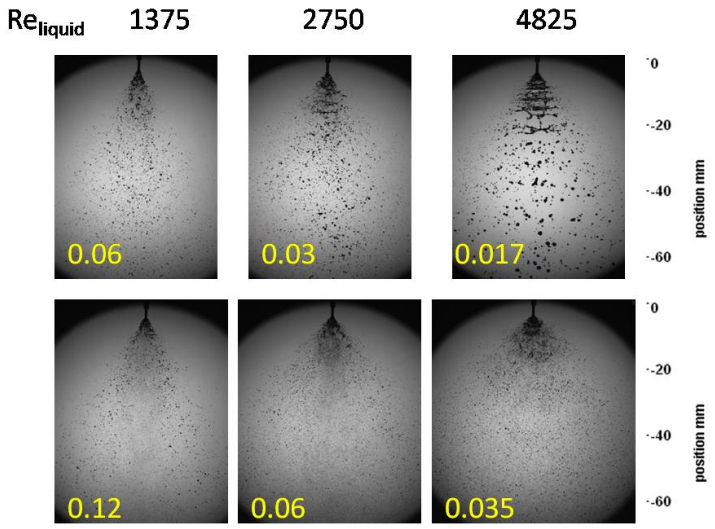

Figure 4. Spray structure at different Gas to Liquid Ratios (GLRs) with a small gas orifice, and impinging angle of 90°.

Injecting the same amount of gas through a small orifice (as opposed to the large orifice) improved the liquid break up further. Figure 4 shows spray structure images at an impinging angle of 90° with a gas orifice of diameter 0.76 mm. Fig. 3 (a) shows sprays from a similar condition but with a larger gas orifice diameter (of 1.1 mm). It is observed that the breakup is more in Fig. 4 due to the fact that reducing the gas orifice size increases the momentum flux of the gas jet. With a smaller gas orifice, the liquid jets break up even before they impinge on each other, when the liquid jet velocity is low.

The effect of the gas is quantified in terms of breakup length at various conditions. Spray structure images are analyzed using an automated computer program. The breakup length is defined as a distance from the impinging point to the point where the liquid jet/sheet continuity breaks. Figure 5 gives a representation of the definition of breakup length. At each condition, the breakup length is obtained for 100 spray images, and the mean and standard deviation are calculated. The breakup length is non-dimensionalised by dividing by the liquid jet orifice diameter. The variation of non-dimensional breakup length with liquid jet Reynolds number at different gas flow rates and impinging angles are plotted and shown in Fig. 6. The standard deviation of 100 images is indicated as the error bar in the plots. In the absence of the gas jet, the breakup length initially increases with an increase in liquid jet velocity and then falls. At low liquid jet velocities, instabilities created by jet impact are not strong enough to break the liquid sheet. An increase in the velocity increases the sheet area due to the higher liquid flow rate, and hence the breakup length. With a further increase in the liquid jet velocity, the breakup length starts decreasing since the instabilities created by impact are strong enough to break the liquid sheet. A gas flow rate of 5 SLPM resulted in reducing the mean breakup length without affecting the trend that is observed at zero gas flow rate. The reduction in the breakup length is more at low liquid jet velocities compared to high velocities of liquid jet. The above observations were noticed for all the impinging angles studied. Increasing the gas flow rate further to 10 SLPM reduced the breakup length significantly. Overall, for all impinging angles, the effect of the gas is higher at low liquid jet velocities and diminished as the velocity was increased.

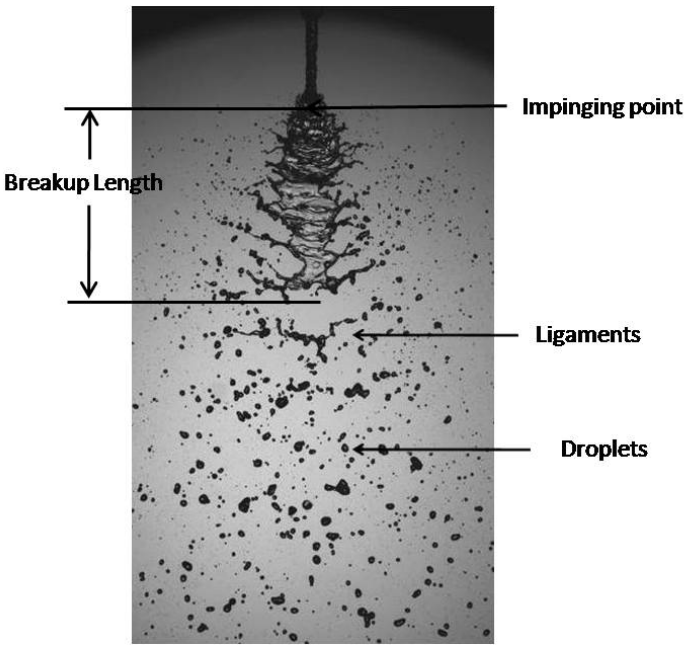

Figure 5. Front view of spray showing breakup length.

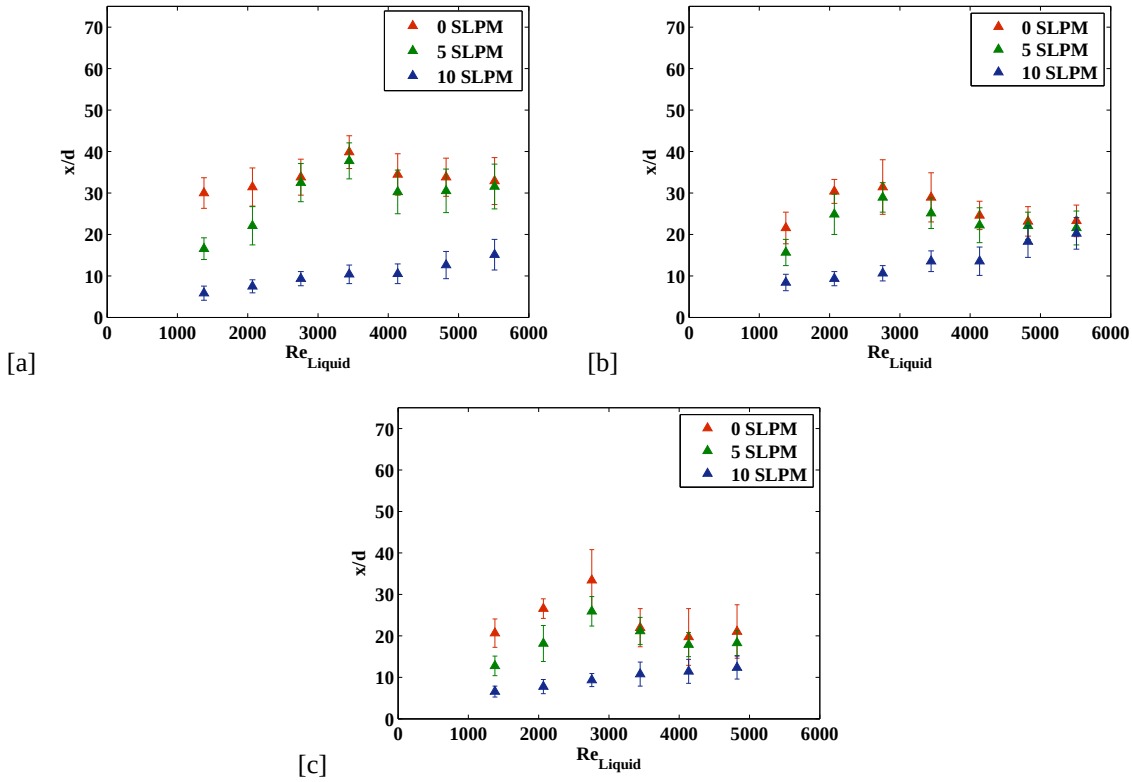

Figure 6. Breakup lengths at (a) 60°, (b) 90°, and (c) 120°, respectively.

Droplet size measurement

Spray droplet sizing measurements are done using PDIA technique at a distance of 75 mm downstream of the impinging point. A 4 mm X 4 mm region of the spray has been imaged, which gives a pixel resolution of 2 μm per pixel.To reduce the error in SMD estimation, droplets which are below 10 μm in size, which corresponds to an area below 25 pixels, are considered as background noise and hence neglected for SMD calculations. A

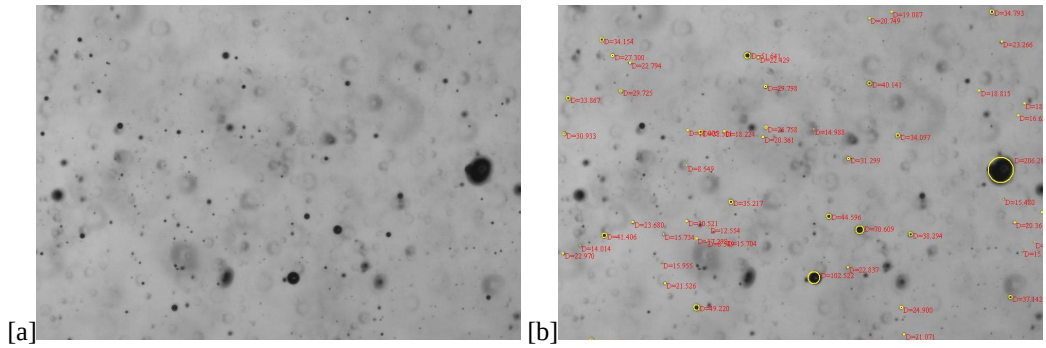

Figure 7. Portion of image analysed for droplet sizing (a) Unprocessed image, and (b) Processed image

total of 400 images at a rate of 10 frames per second were acquired at each condition, to obtain a statistically sufficient number of droplets. The acquired images were analysed using the LaVision Particle Master Shadow module to get the droplet information. Figure 7 shows the portion of the image analysed for droplet sizing before and after processing. Depth of focus calibration was performed using a plate with dots ranging from 10 μm to 200 μm in size. For the settings used in the current study, it was observed that the depth of focus varies from 0.05 mm for 10 μm droplets to 1 mm for 200 μm droplets, and varies linearly between these limits. Droplet sizing measurements are performed at an axial location of 75 mm downstream of the impinging point, at four radial locations which are 10 mm apart starting from the center of spray. Measurements were made at a gas flow rate of 10 SLPM for gas orifice diameters of 1.1 mm and 0.76 mm. To measure the SMD of impinging jets without gas flow, since the droplets are very large, a portion of the spray structure image at 75 mm axial location (taken without the microscope) is analysed.

Results of the droplet sizing at different conditions are shown in Fig. 8. Droplet sizes are very high with only impinging liquid jets and low liquid jet velocity. The SMD reduces from 2.2 mm to 600 μm as the liquid jet velocity is increased, as shown in Fig. 8(a). Figure 8(b) shows the variation of SMD of the spray using a 1.1 mm gas orifice. Droplet sizes are observed to increase with an increase in the liquid jet velocity. A variation in the droplet size with radial location is also observed. Droplet diameters are highest at the center and reduce as one moves towards the edge of the spray radially. This variation in the SMD increased with an increase in the liquid jet velocity. Reducing the gas orifice diameter to 0.76 mm showned a further reduction in the SMD as observed in Fig. 8(c). The trends of variation of SMD with liquid jet velocity are similar to the 1.1 mm gas orifice. However, the variation of SMD with radial location is opposite to that seen earlier, with larger droplets at the edges and smaller droplets at the center. Further, the difference in the SMD of the spray at different radial locations is found to reduce at higher liquid jet velocity, which is also opposite to the trend observed in the 1.1 mm gas orifice case. This difference is due to the fact that with a smaller gas orifice, liquid jets are broken completely before they impinge on each other.

Summary and Conclusions

Spray characteristics of an air-assisted impinging jet atomizer have been studied at various conditions using water as the liquid and nitrogen as the atomizing gas. Introducing gas on top of the impinging point of the liquid jets was found to improve the atomization. Increasing the gas flow rate showed a reduction in the breakup length of the sheet. Further, at the same gas flow rate, using a smaller gas injection orifice resulted in better atomization and the spray was confined to smaller region. At the same liquid and gas flow rates, the method of placing the air injector between the liquid jets improved the atomization significantly compared to blasting a single liquid jet with two air jets.

Droplet size measurements at a distance of 75 mm downstream of impinging point showed a reduction in droplet size with the introduction of the gas jet, while increasing the liquid jet velocity was found to increase the droplet size. Variation in the droplet size was observed with radial distance, and this variation increased with increase in the liquid jet velocity with a 1.1 mm gas orifice but reduced with a 0.76 mm gas orifice. Using a smaller gas injection orifice was observed to break up the liquid jets before they impinge, and resulted in smaller droplet sizes at the center of the spray compared to at the edges. This phenomenon was observed especially at low liquid jet velocities. Overall, the experimental results show that the momentum flux of the gas jet plays an important role in liquid jet breakup. Increasing the momentum flux either by increasing the gas flow rate or by reducing the gas orifice diameter results in improved breakup.

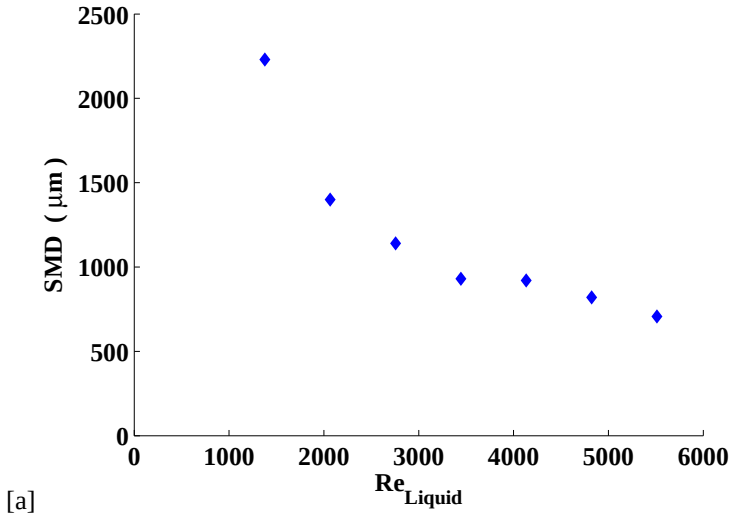

[a]

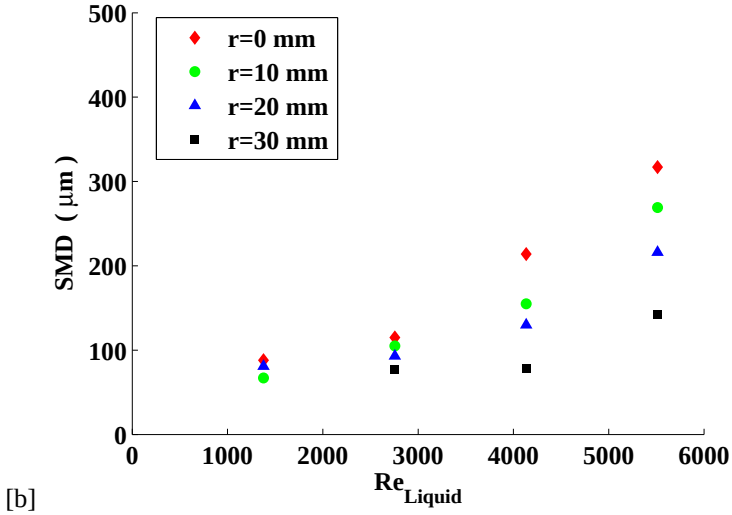

[b]

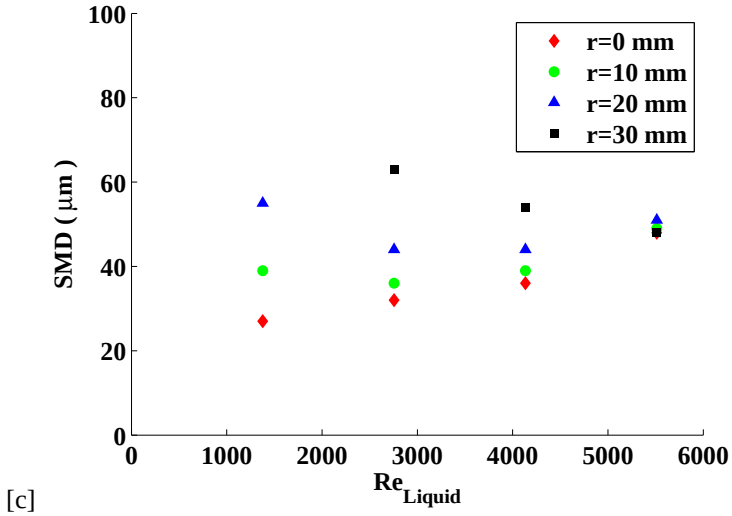

[c]

Figure 8. Sauter mean diameter at various liquid flow rates and radial locations (a) Without gas, (b) with 1.1 mm Gas orifice, and (c) with 0.76 mm gas orifice

References

[1] Lefebvre, A. W., *Gas Turbine Combustion* McGraw-Hill Publications 213 (1983).
[2] Tsai, S. C., Viers, B., *Fuel* 69:1412-1419 (1990).
[3] Buckner, H. N., Sojka, P. E., *Atomization and Sprays* 1:239-252 (1991).
[4] Beck, J. E., Lefebvre, A. E., Koblish, T. R., *Atomization and Sprays* 1:155-170 (1991).
[5] Ibrahim, E. A.,Przekwas, *Physics of Fluids* 12:2981-2987 (1991).
[6] Bailardi, G, Negri, M., Ciezki, H. K. *Proc. 23rd European Conference on Liquid Atomization and Spray Systems, Brno, Czeck Republics*, 2010.
[7] Shen Y., Mitts C.,Poulikakos D., *Atomization and Sprays* 7:123-142 (1997).
[8] Yule, A. J., Chiger, N. A., Cox, N. W., *Particle Size Analysis* 61-73 (1978).
[9] Kim, K. S., Kim, S. S.,*Atomization and Sprays* 4-1:65-74 (1994).
[10] Koh, K. U., Kim, J. Y., Lee, S. Y., *Atomization and Sprays* 11-4: 317-333 (2001).
[11] Blaisot, J. B., Yon, J., *Experiments in Fluids* 39: 977-994 (2005).
[12] Esmail, M., Kawahara, N.,Tomita, E., Sumida, M., *Measurement Science and Technology* 21-7: 317-333 (2010).
[13] Kashdan, J. T., Shrimpton, J. S., Whybrew, A., *Particle & Particle Systems Characterization* 21-1: 15-23 (2004).
[14] Kashdan, J. T., Shrimpton, J. S., Whybrew, A., *Particle & Particle Systems Characterization* 20: 387-397 (2003).
[15] Kashdan, J. T., Shrimpton, J. S., Whybrew, A., *Optics and Lasers in Engineering* 45: 106-115 (2007).